Quasi-harmonicity and power spectra in the FPU model

2000 J. Phys. A: Math. Gen. 33 831

(http://iopscience.iop.org/0305-4470/33/5/301)

J. Phys. A: Math. Gen. **33** (2000) 831–839. Printed in the UK PII: S0305-4470(00)06034-0

Quasi-harmonicity and power spectra in the FPU model

Carlo Alabiso†‡ and Mario Casartelli†§

† Dipartimento di Fisica dell'Università, Parco Area Scienze 7a, 43100 PR, Italy
‡ INFN Gruppo collegato di Parma, Parma, Italy
§ Istituto Nazionale di Fisica della Materia, Parma, Italy

E-mail: alabiso@fis.unipr.it and casartelli@fis.unipr.it

Received 15 July 1999, in final form 22 November 1999

Abstract. We evaluate the power spectra of the time series for the following simple observables in the Fermi–Pasta–Ulam model: harmonic energy, kinetic energy, microcanonical density, Frenet–Serret curvature and the Lyapunov variable. For some of these observables, also in the stochastic regime, the spectra show a well defined quasi-harmonic structure, with harmonic frequencies shifted with a single rescaling factor, as calculated in a previous paper. Even higher frequencies are excited: as replicas of the harmonic window at low energy, to end up with a smooth distribution at high energy, showing a power law behaviour (flicker noise). In the intermediate region the shape depends on the observables, but in all cases the crossover is the maximum of the shifted harmonic spectrum. This establishes an intrinsic short-time scale depending only on the energy density, as does the frequency rescaling factor. For the curvature, we also evaluate the standard deviation: above threshold, at increasing energy, it decreases exactly as the inverse of the rescaling factor. This can be interpreted as a focalization around 'effective tori' of a harmonic-like regime which apparently coexist with the chaotic motion.

The Fermi–Pasta–Ulam (FPU) anharmonic chain has been extensively used to clarify the transition between two regimes of motion, hereafter indicated, for simplicity, as ordered and stochastic [1–5]. For details about the model and the parameters, see [2]. Here we only give the form of the Lagrangian function:

$$\mathcal{L} = \sum_{i=1}^{N} \left[\frac{1}{2}(\dot{x}_i^2 - \chi (x_{i+1} - x_i)^2) - \frac{\varepsilon}{4}(x_{i+1} - x_i)^4 \right] \qquad x_{N+1} = x_1. \tag{1}$$

It has been well established that the energy density $u = E/N$ (where E is the total energy and N the number of particles in the chain), is an order parameter with a transition band (u_1, u_2) such that the motion is ordered for $u < u_1$ and stochastic for $u > u_2$. The very nature of such a transition may be interpreted as follows:

- as a weak-chaos/strong-chaos transition, by looking at the ordered regime as an extremely slow approach to equilibrium (see e.g. [3, 5–7]);
- as a transition from order to stochasticity, by emphasizing the possible role of surviving invariant surfaces (see e.g. [1, 2, 8]). Residual surfaces, or quasi-constants of motion, even if with zero-measure, could also provide a certain degree of order within the stochastic regime.

0305-4470/00/050831+09$30.00

These two points of view are not necessarily incompatible. In fact, the first one stresses the role of long times in the settlement of disorder, while the second stresses the role of structural properties, linking the dynamics and local geometrical features of trajectories, even appearing within short evolution times. In this paper we shall deal mainly with the second approach, exploring the possible existence of an intrinsic short-time scale. To this end, we have studied the spectral properties of time series for some simple observables, measured at discretized times $t = n\hat{t}$, $\hat{t}$ being the sampling interval. The observables are:

- the total harmonic energy

$$E^h = \tfrac{1}{2}\sum_{k=1}^{N} \omega_k (p_k^2 + q_k^2) = \sum_{k=1}^{N} E_k \tag{2}$$

  expressed in terms of the canonical homogeneous variables $(\boldsymbol{p}, \boldsymbol{q})$, which diagonalize the harmonic part of (1) as in [2]. We have also considered separately, when necessary, the plain kinetic energy T;
- the microcanonical density $\rho(t) = 1/|\nabla H(t)|$;
- the Frenet–Serret first curvature $\kappa(t)$;
- the local rate of divergence, or 'Lyapunov observable', $\delta_n = \delta(\hat{t}, n)$.

All these observables have been previously used, in various ways and forms, to approach the transition problem described above. In explicit terms the curvature $\kappa(t)$ is defined by the first Frenet–Serret formula [2]

$$\frac{\mathrm{d}\boldsymbol{t}}{\mathrm{d}s} = \kappa \boldsymbol{n} \tag{3}$$

where $\boldsymbol{t}$ and $\boldsymbol{n}$ are the tangent and normal unitary vectors to the trajectory, and s is the curvilinear coordinate. As for the last quantity δ_n, we recall that, in suitable limits, its time average gives the largest Lyapunov exponent [9]. Its definition is as follows: at time $t = 0$ consider two orbits displaced by a vector $\boldsymbol{D}(0)$ at small distance $D_0 = |\boldsymbol{D}(0)|$. Let them evolve for a time $\hat{t}$ and evaluate the new displacement $\boldsymbol{D}(\hat{t})$ and the distance $D_{\hat{t}}$; then, renormalize the position of the second orbit multiplying $\boldsymbol{D}(\hat{t})$ by $D_0/D_{\hat{t}}$. This procedure may be iterated. At the nth iteration (or time $t = n\hat{t}$) it provides the distance $D_{n\hat{t}}$. Then $\delta_n = 1/\hat{t}\log(D_{n\hat{t}}/D_0)$. Actually, the above procedure is only an approximation to the correct definition of the maximal Lyapunov exponent, which should be calculated in the tangent manifold to each point. The validity of this approximation for our needs has been established by looking at the stability of the results when $\hat{t}$ tends to zero in numerical experiments. In any case, δ_n measures the local divergence of trajectories.

By numerical integration of the equation of motion, we have computed the truncated time series $\{f_1, f_2, \ldots, f_m\}$, f being one of our observables, and their power spectra via fast Fourier transform. The analysis of the spectral properties has been completed with the evaluation of the usual statistical quantities, such as time averages and standard deviations along the orbit. For observables with an intrinsic geometrical meaning (such as κ), we also expect that these quantities provide a link between geometry and dynamics.

Before introducing the results, we give some experimental specifications.

- N: in most experiments $N = 64$, with several checks up to $N = 512$.
- m, the length of the time series: we have chosen $m = 2048, 4096, 8192$, with checks up to $m = 32\,768$. Apart from obvious differences, different m give coherent results even above threshold. Note that these times are very short with respect to usual thermalization times [7, 8].

- $\hat{t}$, the Lyapunov free-evolution time: we have chosen $\hat{t} = 50\Delta t$, where $\Delta t = 0.0024$ is the integration step, or equivalently $\hat{t} = 0.382\tau_{\min}$, where $\tau_{\min}$ is the shortest harmonic period. Experiments with $\hat{t} = 25\Delta t$ or $100\Delta t$ confirmed the stability and reliability of the results.
- The sampling interval: for simplicity, we have chosen the same $\hat{t}$ value as above. The results have been proven independent of it, at least qualitatively.
- u: we have spanned the interval $0.001 < u < 100$, the transition band ranging from $u_1 = 0.1$ to $u_2 = 1.0$.
- Initial conditions: we have chosen random values for the canonical variables $(\boldsymbol{p}, \boldsymbol{q})$.
- Initial displacement $\boldsymbol{D}(0)$ of the second orbit, chosen in a random direction with length $D_0 = 10^{-7}$.
- Transient T_0: before starting the sampling of our quantities, we let the system evolve freely for a transient, in order to reduce the bias from initial conditions and displacements. In most experiments, the transient has been chosen 75 or 375 times the longest harmonic period, with checks up to 1900 times.
- Numerical integration: a standard fifth-order Runge–Kutta routine was used, with the integration step Δt mentioned above, sufficient for good energy conservation (one part in 10^7 in the worst conditions).

The results may be summarized as follows: at all energies, below, through and above threshold, the frequencies in the power spectra may be divided in two distinct intervals, which define a crossover angular frequency ω^*, and consequently a period $\tau^* = 2\pi/\omega^*$. Figures 1–6 exhibit the ways in which this crossover frequency appears for different observables at different energies. This frequency depends on the energy density u, but is the same for all observables and for all the examined numbers N of degrees of freedom. In particular, we stress that the peak around ω^* does not depend on N, and it cannot be explained by the accumulation of more and more frequencies when N grows. Indeed, single peaks may always be discriminated by looking at single E_k.

The general features of the two frequency intervals are:

(1) Below ω^*. Particularly for E^h and ρ (whose spectra are very similar also in details) the first frequency interval presents a whole set of peaks recognizable as a rescaled harmonic spectrum, whose maximal frequency is just given by ω^*. We call the frequency interval up to ω^* the 'quasi-harmonic window', or the 'main window'. This occurs below and above the stochasticity threshold. We recall that the existence of a quasi-harmonic frequency spectrum even above threshold was already established analytically in [1]. The expression for it, which is very precisely checked by our present numerical experiments, is the following:

$$\tilde{\omega}_k = \tilde{\alpha}\omega_k \qquad \text{where} \quad \tilde{\alpha} = (1+\alpha)^{1/2} \qquad \text{and} \qquad \alpha = \tfrac{2}{3}[(1 + 3A\varepsilon u/\chi^2)^{1/2} - 1] \tag{4}$$

where

$$\omega_k = 2\sqrt{\chi}\sin\left(\frac{(k-1)\pi}{N}\right)$$

is the harmonic spectrum, χ and ε are the harmonic and anharmonic strengths, respectively, and A is a correlation parameter, whose experimental value is 2.9 below threshold, and 2.3 above. The rescaling factor $\tilde{\alpha}$ is independent of k and, in our experiments ($\chi = 1, \varepsilon = 0.1$), ranges from 1.00 ($u = 0.001$) to 2.41 ($u = 100$).

While the existence of quasi-harmonic frequencies is in a sense obvious below threshold for the harmonic energy $E^h = \sum_k E_k$, because of its separable structure, it is not quite so obvious at high energies. Moreover, at all energies, it is not obvious for those global observables, such as ρ, that do not possess a simple separable structure.

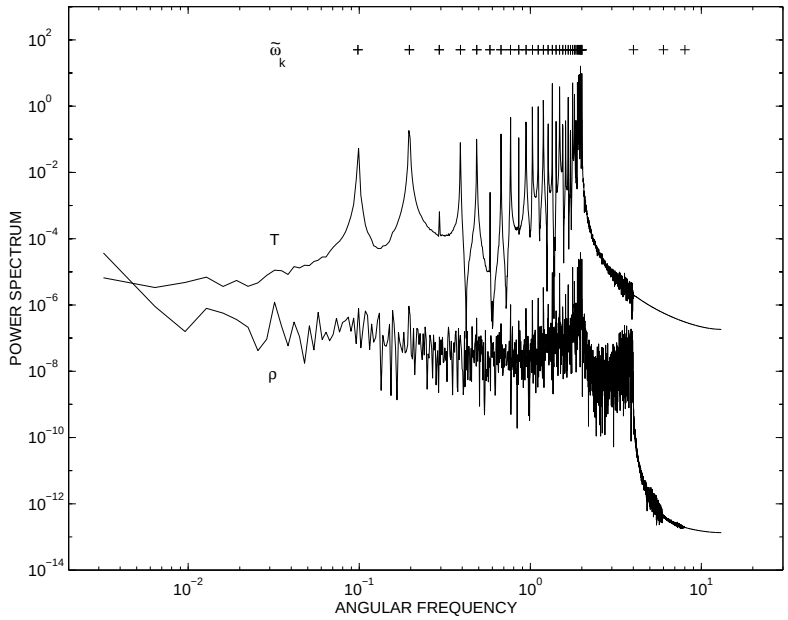

Figure 1. Power spectra with $u = 0.01$ for kinetic energy (T) and microcanonical density (ρ). The harmonic frequencies ω_k are rescaled according to equation (4). Extra frequencies mark 2, 3, 4 times the maximal $\tilde{\omega}_k$ (ω^*). T is multiplied by a factor of 10 for graphical reasons.

We note also that, below threshold, single harmonic energies E_k are quasi-constant of motion, and consequently their signals in the Fourier transform of E^h are mostly constituted by noise. Therefore, to give evidence to the shifted frequencies, it is convenient to study the kinetic components $\frac{1}{2}\omega_k p_k^2$, or else their sum T which is not constant at all, as shown in figures 1 and 3.

(2) Above ω^*. All frequencies are also excited (up to the maximum compatible with the sampling) with a pattern depending on the energy u. Going through figures 1 and 3, or figures 2 and 4, we see the onset of excited bands, whose maxima are multiples of ω^*, indicated with additional plus marks in the figures. We call these frequency bands 'secondary windows'. Their number is growing with u, and their intensity at fixed u is rapidly decreasing. In the stochastic regime, the secondary windows collapse into a continuous descent, shown in figures 5 and 6, where only the first of the secondary windows preserves a certain individuality (this is particularly true for κ). The general behaviour, more and more evident as the energy grows, is a linear descent in the log–log scale, i.e. a negative power behaviour $1/\omega^a$ (coloured or flicker noise). The exponent a is similar for E^h and ρ, but slightly different for δ and κ. The frequency-distribution shape around ω^* depends on the observables, but the evidence of the crossover frequency is always very clear. Apart from the peaks, we do not have any clear indication about the noise superimposed on the quasi-harmonic spectrum in the main window.

Besides these general features, some observables have peculiar behaviours, as discussed in the two following paragraphs.

The Lyapunov δ requires, below threshold, an extremely long transient to reach a stable spectrum, probably due to the slow settlement of the second orbit; furthermore, once stabilized, this spectrum is almost exclusively composed of noise, showing a little evidence for ω^*

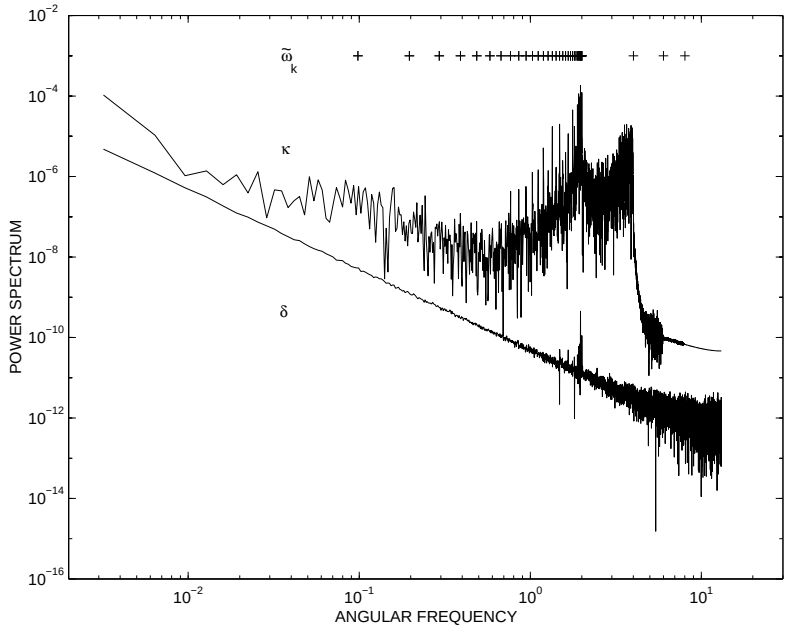

Figure 2. Spectra with $u = 0.01$ for Lyapunov term (δ), and Frenet–Serret curvature (κ). The observable δ is multiplied by a factor of 10^4.

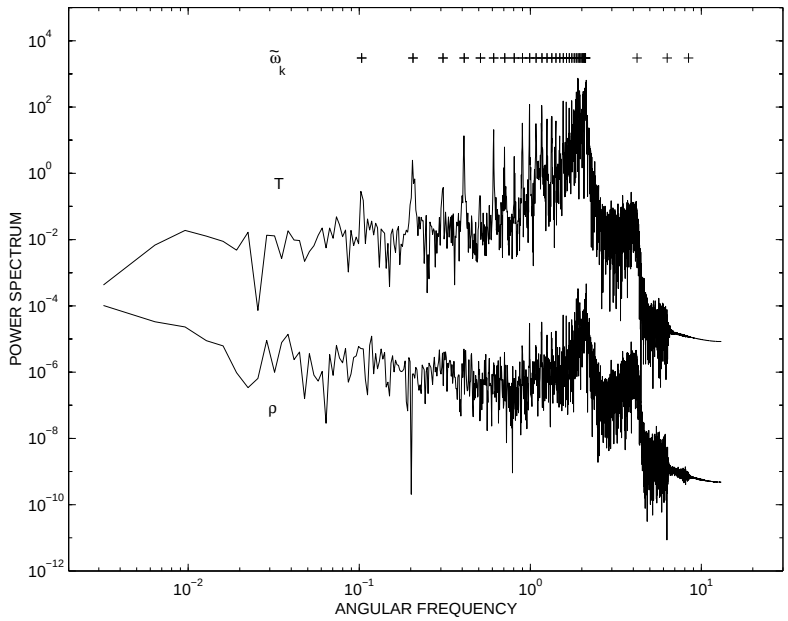

Figure 3. Spectra with $u = 0.4$ for kinetic energy (T) and microcanonical density (ρ).

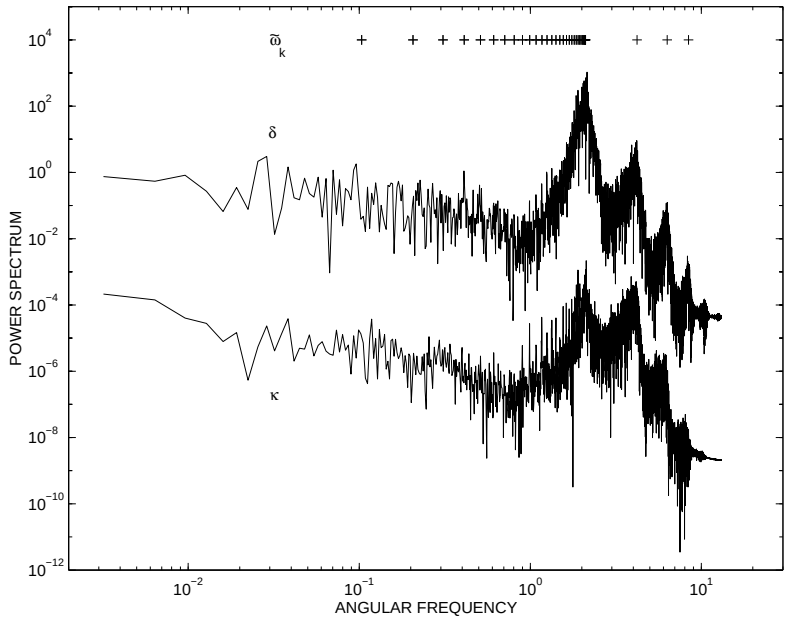

Figure 4. Spectra with $u = 0.4$ for Lyapunov term (δ) and Frenet–Serret curvature (κ). The observable δ is multiplied by a factor of 10^2.

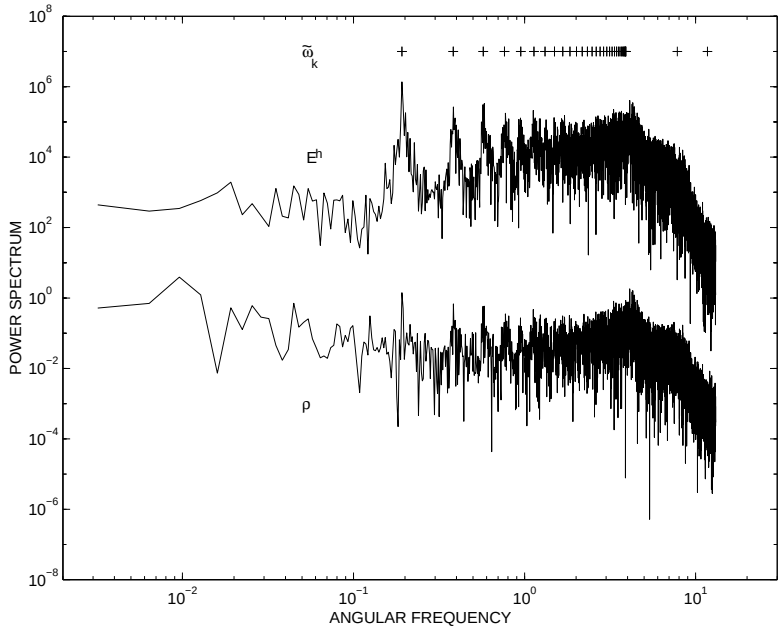

Figure 5. Spectra with $u = 40$ for harmonic energy (E^h) and microcanonical density (ρ), multiplied by a factor of 10^5.

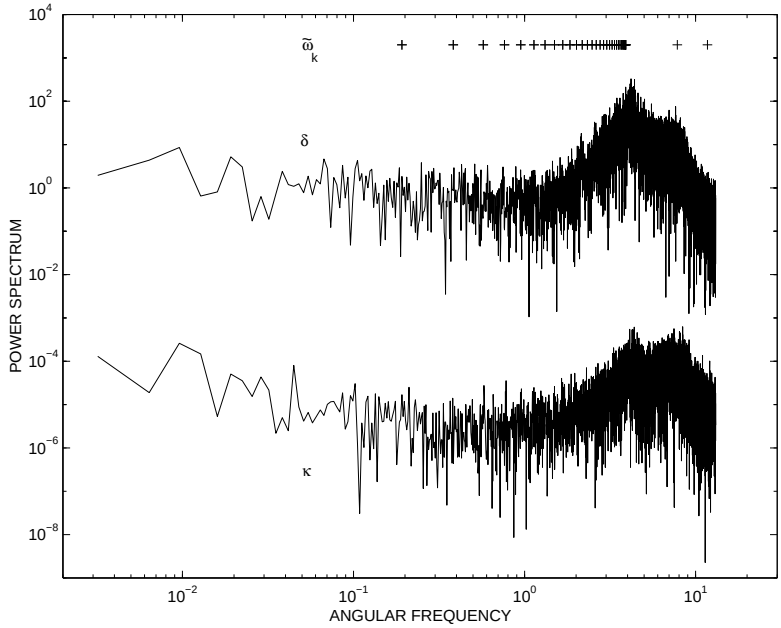

Figure 6. Spectra with $u = 40$ for Lyapunov term (δ) and Frenet–Serret curvature (κ). The observable δ is multiplied by a factor of 10.

(figure 2). Growing with energy, the transient time for δ is drastically shortened, and even for this observable the overall pattern provides very clear evidence for ω^*, as shown in figures 4 and 6, through a strong enhancement even of the frequencies around ω^*. In the log–log scale, the peak around ω^* seems to be at the confluence of two power laws inverse to each other. The same enhancement holds for κ in a weaker way.

Another remarkable point regards $STD(\kappa)$, the standard deviation of the curvature along the orbit, whose behaviour versus u is shown by the lower curve in figure 7. Recalling that in the homogeneous variables $(\boldsymbol{p}, \boldsymbol{q})$ the purely harmonic κ is a constant of motion, and therefore $STD(\kappa) = 0$ in the harmonic limit, the initial growth up to threshold is obviously due to the growing dispersion of values along the trajectory. However, after threshold, this trend is reversed: $STD(\kappa)$ decreases, i.e. there is a progressive focalization of the observable around its mean value. In this sense, we find again that stochasticity coexists with a more and more stable harmonic-like behaviour. How the standard deviation decreases above threshold is shown by the upper curve, which represents the same quantity multiplied by $\tilde{\alpha}$, the rescaling factor. It tends to be constant, which means that the standard deviation behaves as $\tilde{\alpha}^{-1}$. So far, however, this is only an empirical observation confirming the peculiarity of the curvature as a link between geometry and dynamics [2].

Conclusions

The structure of the main window shows that, even above threshold, the single quasi-harmonic modes retain their individuality, not contrasting the final thermalization.

The flicker noise, a phenomenon emerging at high energies for all observables as discussed in point (2), relates to short correlation times $t < \tau^*$. This should not be influencial on the

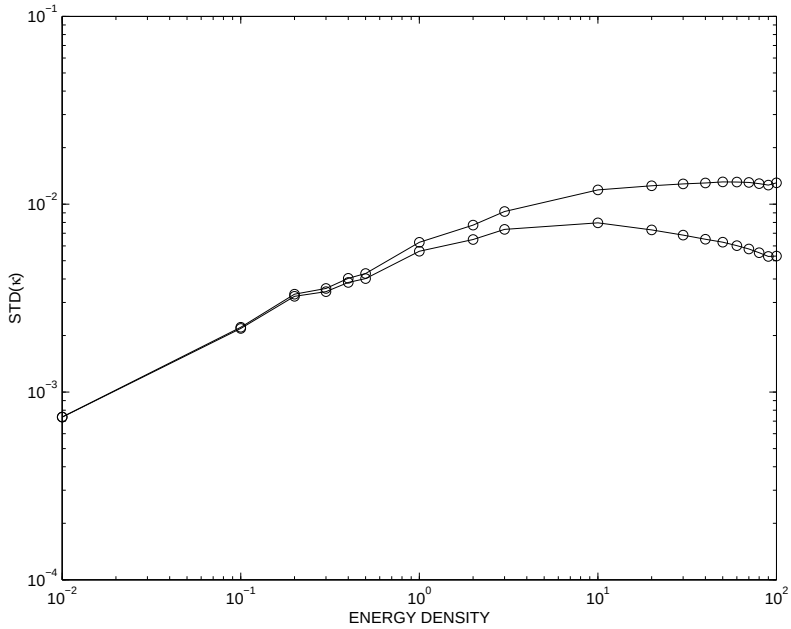

Figure 7. Lower curve, the standard deviation of the time series of the Frenet–Serret curvature κ, as a function of specific energy u. Upper curve, the same multiplied by the factor $\tilde{\alpha}$ given in (4).

problem of thermalization seen as the problem of asymptotic averaging of any observables. The self-similarity in time, implied by flicker noise, has a preview below and through threshold in the onset of secondary windows.

The crossover frequency ω^* depends only on the order parameter u. This supports the physical relevance of $\tau^* = 2\pi/\omega^*$ as the intrinsic short timescale of the model, which should properly substitute the purely harmonic timescale $1/\omega_{\max}$ of common use. However, the rescaling factor grows, at most, to a few units in the large range we explored, and this explains why the usual reasoning based on a purely harmonic timescale retains its practical validity even above threshold.

The persistence of harmonic-like features within stochasticity is also indicated by the behaviour of the standard deviation of κ, which decreases at growing energies: as stated, this implies the focalization of κ around its mean value. In geometrical terms, complementary to dynamics, this may be viewed in the following way: in the phase space there persist fundamental oscillations remembering the original harmonic motion on the tori, whose trace is the quasi-harmonic spectrum. Motion takes place, in the mean, on such 'effective tori', and the return of $STD(\kappa)$ to harmonic-like behaviour as energy grows is due to the stabilization of these tori. Furthermore, there are also small secondary oscillations of high frequency, corresponding to additional small deformations of the trajectories. As for the geometrical pattern of these small deformations, since we know that high frequencies follow a power law pattern, it is plausible that the deformations, as the geometrical counterpart of this coloured queue, tend to a sort of fractality. Of course, there is no breaking of smoothness and such a fractality is to be intended within the same type of approximation in which we speak of flicker noise.

Here we have overlooked asymptotically long times, linked with the approach to

equilibrium of the isolated system. We stress that, for the main window, the independence of N we have observed relates to the existence and the localization of quasi-harmonic peaks, not to details of their shapes which, differently than in the secondary windows, could depend on the slow relaxation of the long-wavelength modes, depending in turn on N (compare the discussion and, in particular, figure 1 in [1]). In [10, 11] it has been suggested that this slow relaxation may influence the behaviour of physically meaningful features, e.g. thermal conductivity, for both isolated and non-isolated one-dimensional chains. We do not know if the short time structure may also be significant in this respect. In fact, we observe that in figure 2 of [11], the power spectrum of the global heat flux in FPU chains also shows two distinct regions, with a crossover between two power laws: there is a remarkable agreement with our spectra in the high-frequency region, a neat difference in the low-frequency one, where they observe a divergence. Moreover, the crossover frequency does not recover, apparently, the role of our ω^*. Therefore the link, if any, between these kind of physical properties and the short time structure we have explored, is not obvious.

References

[1] Alabiso C, Casartelli M and Marenzoni P 1995 *J. Stat. Phys.* **79** 451
[2] Alabiso C, Besagni N, Casartelli M and Marenzoni P 1996 *J. Phys. A: Math. Gen.* **29** 3733
Alabiso C and Casartelli M 1997 *J. Phys. A: Math. Gen.* **30** 7009
[3] Pettini M and Landolfi M 1990 *Phys. Rev.* A **41** 768
Pettini M and Cerruti-Sola M 1991 *Phys. Rev.* A **44** 975
[4] Kantz H, Livi R and Ruffo S 1994 *J. Stat. Phys.* **76** 627
[5] Casetti L, Livi R and Pettini M 1995 *Phys. Rev. Lett.* **74** 375
[6] De Luca J, Lichtenberg A J and Lieberman M A 1995 *Chaos* **5** 283
[7] Parisi G 1997 *Europhys. Lett.* **40** 357
[8] Alabiso C, Casartelli M and Marenzoni P 1993 *Phys. Lett.* A **183** 305
[9] Benettin G, Galgani L and Strelcyn J M 1976 *Phys. Rev.* A **14** 2338
[10] Lepri S, Livi R and Politi A 1997 *Phys. Rev. Lett.* **78** 1896
Lepri S, Livi R and Politi A 1998 *Physica* D **119** 140
Lippi A and Livi R *Preprint* chao-dyn 99100341
[11] Lepri S, Livi R and Politi A 1998 *Europhys. Lett.* **43** 271